Electronic Supplementary Information

Hydrogels Endow the Precise Growth Tracks of Plasmonic Gold Nanoparticles for Mercury Analysis

Hang Zhang, Jun Jiang Luo, Zhe Sun, Hao Lin Zou, Hong Qun Luo, Nian Bing Li,*
Bang Lin Li*

Key Laboratory of Luminescence Analysis and Molecular Sensing (Southwest University), Ministry of Education, School of Chemistry and Chemical Engineering, Southwest University, Chongqing 400715, P. R. China.

Email: chemlibl@swu.edu.cn (B. L. Li); linb@swu.edu.cn (N. B. Li)

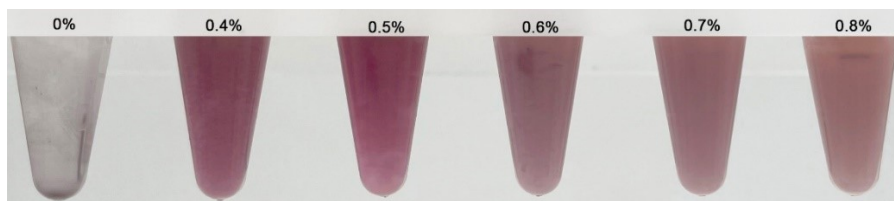**This PDF file includes seven figures, two tables, and nine pages:**

Figure S1.

Fig. S1. The pictures showing the different nano-staining reactions of HAuCl$_4$ and cysteine in various concentrations of agarose. The concentrations of cysteine, HAuCl$_4$ and Hg^{2+} ions were 0.2 mM, 1.0 mM and 100 nM, respectively.
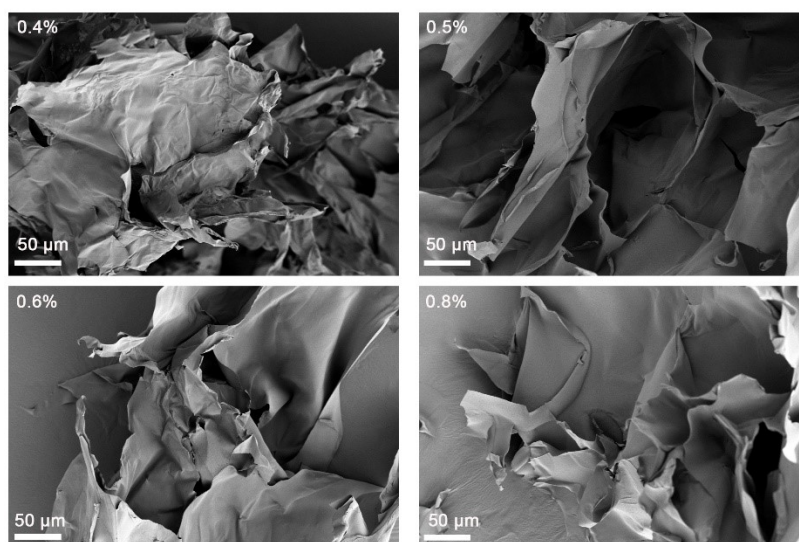
Figure S2.

Fig. S2. Scanning electronic microscope (SEM) pictures showing the diversity of pore sizes in hydrogels which are prepared from different concentrations of agarose (0.4%, 0.5%, 0.6%, 0.8%).
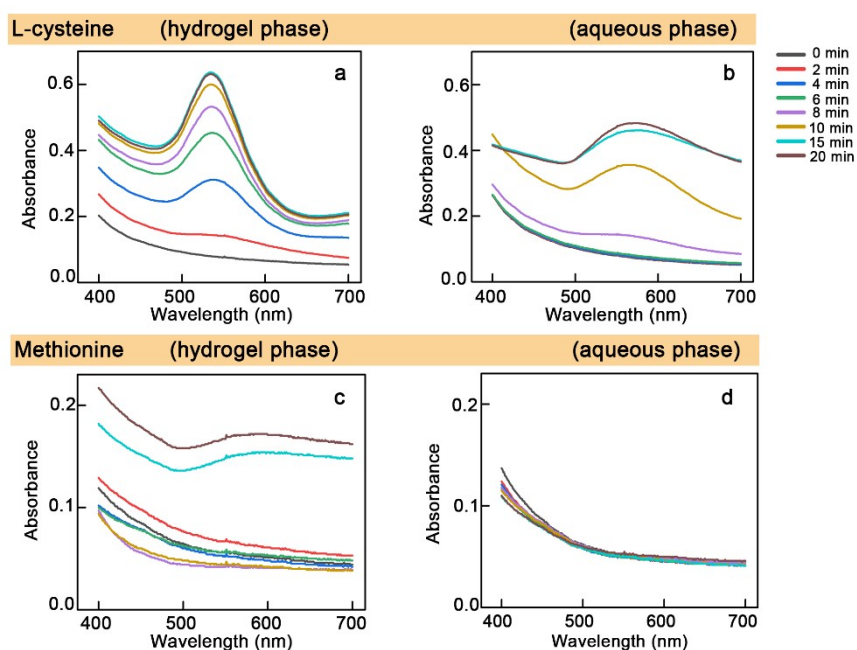
Figure S3.

Fig. S3. Time-resolved absorption spectra for recording the formation process of gold NPs with different reduction reagents of L-cysteine (a, b) and methionine (c, d) in agarose hydrogel (a, c) and aqueous (b, d) phases. The concentrations of L-cysteine and methionine are 0.5 mM.
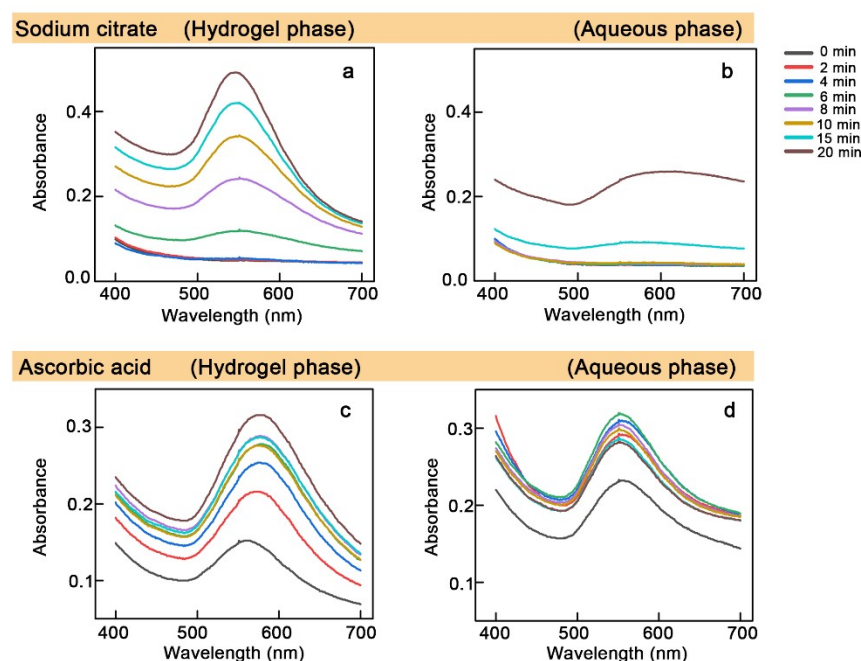
Figure S4.

Fig. S4. Time-resolved absorption spectra for recording the formation process of gold NPs with different reduction reagents of sodium citrate (a, b) and ascorbic acid (c, d) in agarose hydrogel (a, c) and aqueous (b, d) phases. The concentrations of sodium citrate and ascorbic acid are 0.5 mM.

Figure S5.
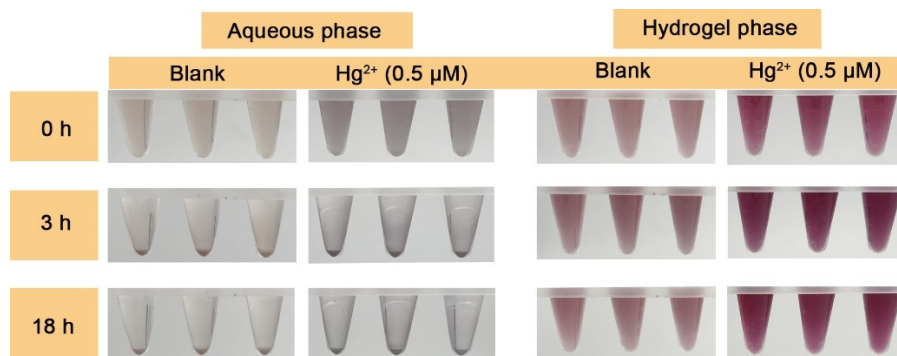

Fig. S5. Real pictures displayed the different growth processes of gold NPs in two reaction phases, which were incubated in the absence and presence of Hg^{2+} ions for diverse standing times (0, 3, and 18 h)

Figure S6.
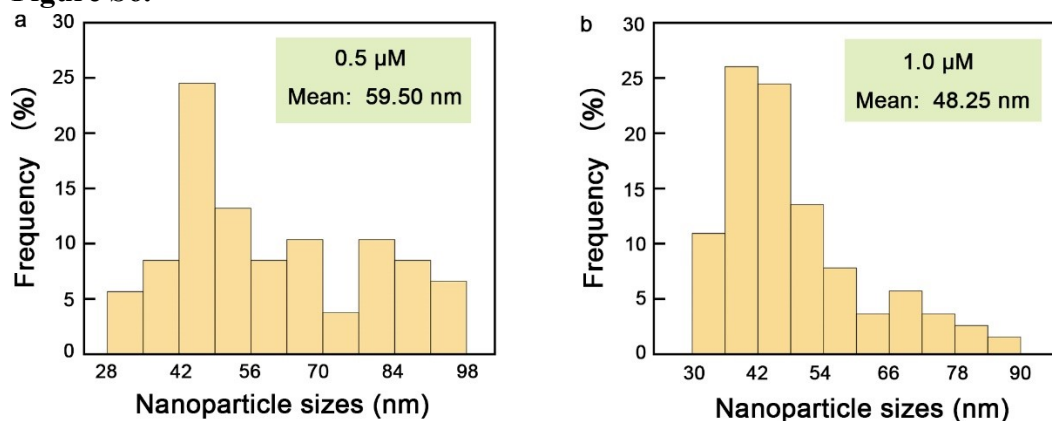
Fig. S6. The size distribution of gold NPs in the nano-staining hydrogels, which are generated from 0.5 µM (a) and 1.0 µM (b) Hg^{2+} ions, respectively.

Figure S7.

Fig. S7. Fourier transform infrared (FTIR) spectra of diverse forms of agarose. (a) the agarose powders. (b) the agarose aerogel. (c) the cysteine doped agarose aerogel. (d) the agarose aerogel after the treatments of nano-staining sensing strategies. The reaction had no effects to the chemical composition of agarose.

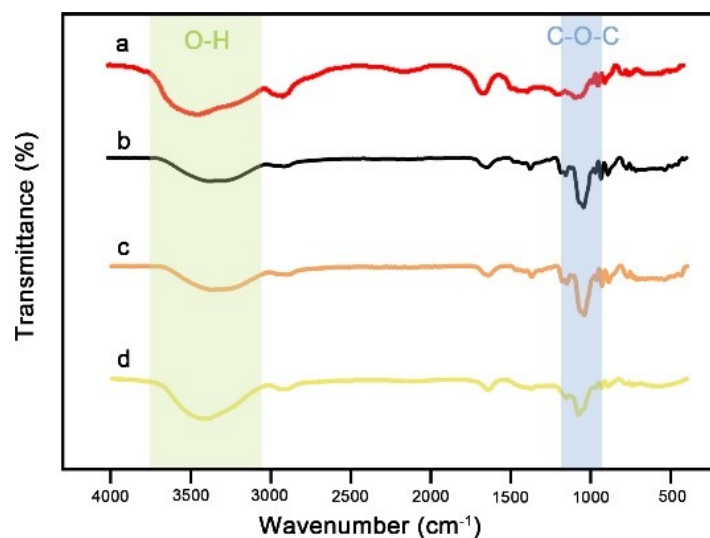**Table S1**. Measurements of Hg^{2+} ions in real samples using the nano-staining hydrogel assay.

Sample [a]	Original concentration (nM)	Added Hg^{2+} concentration (nM) [b]	Nano-staining hydrogel assay (nM) [c]	Recovery (%)	RSD
Tap water	0.00	200.00	194.32	97.16	6.48
	0.00	400.00	465.60	116.40	4.10
	0.00	600.00	555.60	92.60	5.59

[a] Measured five times. [b] Added amount of Hg^{2+} ions in the environmental samples. [c] Measured results based on our developed method.

Table S2. The list indicating the comparison of colorimetric Hg^{2+} analysis routes developed by the plasmonic gold nano-probes.

Response mechanism	Recognition mechanism	Sensing phase	LOD	Other sensing performance (Stability et al.)	Ref.
LSPR of as-prepared AuNP probes	Lysine can strongly interact with Hg^{2+} ions	Aqueous solutions	2.9 nM	Weak, and influenced by the dispersion of nano-probes	Sener et al.[S1]
LSPR of DNA-functionalized AuNP probes	Thymine-Hg^{2+}-thymine coordination chemistry	Aqueous solutions	3.0 µM	Weak, and influenced by DNA modification and dispersion of AuNPs	Xue et al.[S2]
LSPR changes of Au nanobipyramids	The addition of Hg^{2+} induces the formation of a partition layer on Au nanobipyramid surfaces.	Aqueous solutions	200 nM	Weak, and influenced by the dispersion of nano-probes	Qi et al. [S3]
SPR of Ag/Au nanoparticles	Hg^{2+}-induced the specific dissolution of Ag	Aqueous solutions	5 nM	Pb^{2+} ions might interference the analysis results	Xing et al. [S4]
Catalysis of gold amalgam	The electron transfer from mercury to the adsorbed 4-nitrophenol	Aqueous solutions	1.45 nM	The background noise signal was high	Chen et al. [S5]

Mechanism	Chemistry	Substrate	LOD	Stability	Reference
LSPR of as-prepared AuNP probes	Thymine-Hg^{2+}-thymine coordination chemistry	Cellulose paper substrate	50 nM	Weak, and influenced by the dispersion of nano-probes	Chen *et al.* [S6]
Catalytic activity of gold to the reduction of methylene blue	Hg^{2+}-triggered formation of gold amalgam	Porous wood	32 pM	The background noise signal was high	Hai *et al.* [S7]
LSPR of *in-situ* formed AuNPs	High-affinity metallophilic interaction between Hg and Au ions	Agarose hydrogels	3.7 nM	Medium stability which was influenced by the $HAuCl_4$ diffusion	Du *et al.* [S8]
LSPR of *in-situ* formed gold NPs	High-affinity metallophilic interaction between Hg and Au ions	Agarose hydrogels	1.25 nM	High stability independent by reaction times	This work

Supporting References.

[S] G. Sener, L. Uzun and A. Denizli, *Anal. Chem.*, 2014, **86**, 514-520.

[S2] X. Xue, F. Wang and X. Liu, *J. Am. Chem. Soc.*, 2008, **130**, 3244-3245.

[S3] Y. Qi, J. Zhao, G. J. Weng, J. J. Li, X. Li, J. Zhu and J. W. Zhao, *J. Mater. Chem. C*, 2018, **6**, 12283.

[S4] T. Y. Xing, J. Zhao, G. J. Weng, J. J. Li, J. Zhu and J. W. Zhao, *J. Mater. Chem. C*, 2018, **6**, 7557.

[S5] Z. Chen, C. Zhang, Q. Gao, G. Wang, L. Tan and Q. Liao, *Anal. Chem.*, 2015, **87**, 10963-10968.

[S6] G. H. Chen, W. Y. Chen, Y. C. Yen, C. W. Wang, H. T. Chang and C. F. Chen, *Anal. Chem.*, 2014, **86**, 6843-6849.

[S7] J. Hai, F. Chen, J. Su, F. Xu and B. Wang, *Anal. Chem.*, 2018, **90**, 4909-4915.

[S8] X. J. Du, Y. Chen, L. Y. Qin, H. Q. Luo, N. B. Li and B. L. Li, *Environ. Sci. Technol.*, 2022, **56**, 1041-1052.